



[Zhang, J.](#), [Wagih, M.](#) , [Hoare, D.](#), [Mirzai, N.](#), [Mercer, J.](#) , [Das, R.](#) and [Heidari, H.](#) (2023) Highly Integrated and Ultra-Compact Rectenna with Wireless Powering for Implantable Vascular Devices. In: 21st IEEE Interregional NEWCAS Conference (IEEE NEWCAS 2023), Edinburgh, UK, 26-28 June 2023, ISBN 9798350300246 (doi: [10.1109/NEWCAS57931.2023.10198083](https://doi.org/10.1109/NEWCAS57931.2023.10198083))

There may be differences between this version and the published version.  
You are advised to consult the published version if you wish to cite from it.

<https://eprints.gla.ac.uk/299361/>

Deposited on 25 May 2023

Enlighten – Research publications by members of the University of Glasgow  
<http://eprints.gla.ac.uk>

# Highly Integrated and Ultra-Compact Rectenna with Wireless Powering for Implantable Vascular Devices

Jungang Zhang  
Microelectronics Lab (meLAB)  
University of Glasgow  
Glasgow, UK  
j.zhang.8@research.gla.ac.uk

Nosrat Mirzai  
Undergraduate Medical School  
University of Glasgow  
Glasgow, UK  
nosrat.mirzai@glasgow.ac.uk

Hadi Heidari  
Microelectronics Lab (meLAB)  
University of Glasgow  
Glasgow, UK  
Hadi.Heidari@glasgow.ac.uk

Mahmoud Wagih  
Microelectronics Lab (meLAB)  
University of Glasgow  
Glasgow, UK  
mahmoud.wagih@glasgow.ac.uk

John Mercer  
BHF Glasgow Cardiovascular Research  
Centre  
University of Glasgow  
Glasgow, UK  
John.Mercer@glasgow.ac.uk

Daniel Hoare  
BHF Glasgow Cardiovascular Research  
Centre  
University of Glasgow  
Glasgow, UK  
daniel.hoare@glasgow.ac.uk

Rupam Das  
Department of Engineering  
University of Exeter  
Exeter, UK  
r.k.das@exeter.ac.uk

**Abstract**— This paper presents a highly integrated and ultra-compact implantable rectenna for wirelessly powering implantable vascular devices at 1.4 GHz. The proposed implantable rectenna occupies dimensions of  $7 \times 7 \times 0.635 \text{ mm}^3$  and is encapsulated by a biocompatible polydimethylsiloxane (PDMS) package with an overall size of  $8 \times 8 \times 1.635 \text{ mm}^3$ . The miniaturized implantable antenna is achieved by embedding meandered slots on the radiating patch and open-end ground slot. In addition, a single optimized matching inductor is designed for the matching circuit between the antenna and the rectifier. The rectifier is directly integrated into the radiating patch layer of the antenna using a probe feed. The rectifying circuit, utilizing a single-stage voltage doubler topology, efficiently converts radio frequency (RF) power received by the implantable antenna into proper direct current (DC) power to drive the implantable vascular devices. The integrated matching and rectifying circuit are miniaturized to  $4.87 \times 2.05 \times 0.635 \text{ mm}^3$  and exhibits a maximum simulated conversion efficiency of 67.9% with a load resistance of 3 k $\Omega$  at an input power of 7.5 dBm.

**Keywords**—implantable rectenna, wireless powering, impedance matching network, rectifying circuit, implantable vascular devices.

## I. INTRODUCTION

Cardiovascular disease (CVD) is the most significant cause of death in the world. The collective of CVDs includes heart attacks, arrhythmias, and heart failure. Patients suffering from a CVD-related illness nominally have multiple comorbidities such as hypertension, dyslipidaemia, diabetes, or chronic kidney disease [1]. To treat a CVD, implantable medical devices within the vasculature may be used. This could be a coronary or peripheral stent, dialysis graft, or heart valve. These devices can suffer from re-occlusive and thrombotic events which in turn can lead to secondary complications such as strokes and heart attacks [2]. The re-occlusive process is often silent with little to no indication of whether it is to strike. As such researchers, including our group, have developed wireless, self-reporting sensors that

can be combined into vascular implants to detect these re-occlusive complications, presented in Fig. 1. These devices have the ability to revolutionise healthcare through the monitoring of patients 24/7 enabling predictive and pre-emptive treatment before a complication occurs [3].

While we have made significant progress in integrating a sensor with the cardiovascular implant [4] and implementing bidirectional biotelemetry [5], the continuous wireless powering of these devices remains a major technological challenge. Wireless power transfer (WPT) technology has gained enormous attention for battery-free implantable medical devices [6]. Significant research has progressed toward near-field inductive transmission and far-field radiative transmission [7]. Near-field WPT offers relatively higher power transfer efficiency but greatly suffers from short

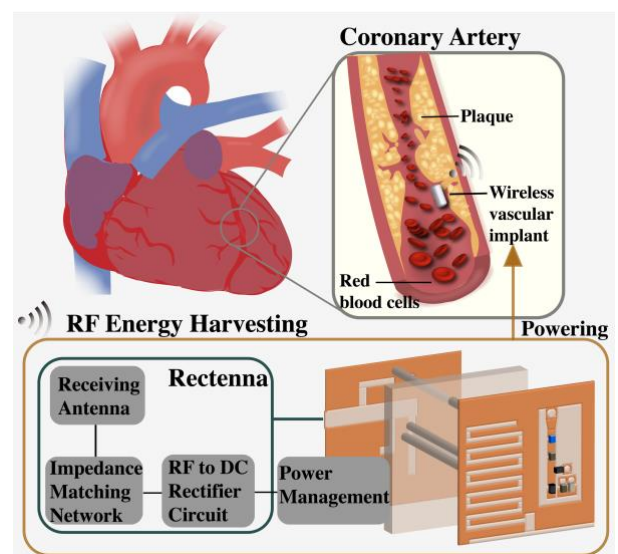


Fig. 1. Overview of the proposed implantable rectenna for implantable vascular devices.

transmission distances and lateral, and angular misalignment. In comparison, far-field WPT is less sensitive to misalignments between the transmitter and receiver over a long distance. Harvesting radio frequency (RF) energy at a far-field distance is a potential solution for removing bulky batteries of implantable medical devices. Implantable rectennas have been massively investigated as the key element for RF energy harvesting systems [8-11]. A rectenna, which receives, stores, and converts the ambient RF power to DC power, consists of an implantable antenna, a rectifier, and along with an impedance matching circuit that uses for maximum power delivery. The design of the implantable rectenna arises many challenges including sufficient power transfer efficiency, compact size, biocompatibility, and high output DC voltage. Particularly, ultra-miniaturization is the barrier and urgent demand for wireless powering implantable devices without detriment to their performance. To our best knowledge, the proposed rectenna is the smallest implantable rectenna with an exceptional performance in the literature, as shown in Table I. We chose a voltage doubler topology as the rectifier since it generates higher output voltage than a shunt diode or series diode, and it also has higher power transfer efficiency compared to a multi-stage multiplier. Additionally, a matching circuit is designed here to maximize the amount of transferred power and reduce the power loss between the antenna and the rectifier circuit. The matching network and rectifier circuit characteristics have been optimized by using Keysight advanced design system (ADS) software in this paper. Besides, a co-simulation of the integrated rectenna configuration is simulated and analysed in this paper. Moreover, the rectenna is simulated in an insulating container material polydimethylsiloxane (PDMS) for the biocompatibility purpose.

As shown in Fig.1, a highly integrated and ultra-compact implantable rectenna is presented, in which the designed antenna and rectifier circuit share a common ground, resulting in a miniaturized size of  $7 \times 7 \times 0.635 \text{ mm}^3$ . The proposed antenna is designed as an RF power receiver and combines with a high frequency rectifier that serves at 1.4 GHz Wireless Medical Telemetry Service (WMTS) for powering implantable vascular implants wirelessly. Besides, a voltage doubler topology is adopted in the rectifier circuit to fulfill the high DC voltage output (3-5 V) required by the implantable vascular devices, which consist of a microprocessor, biosensors, and other ICs for stable operation [12]. The matching network and rectifier circuits were simulated using Keysight ADS software, while the implantable antenna, and integrated rectenna were simulated by Ansys HFSS software.

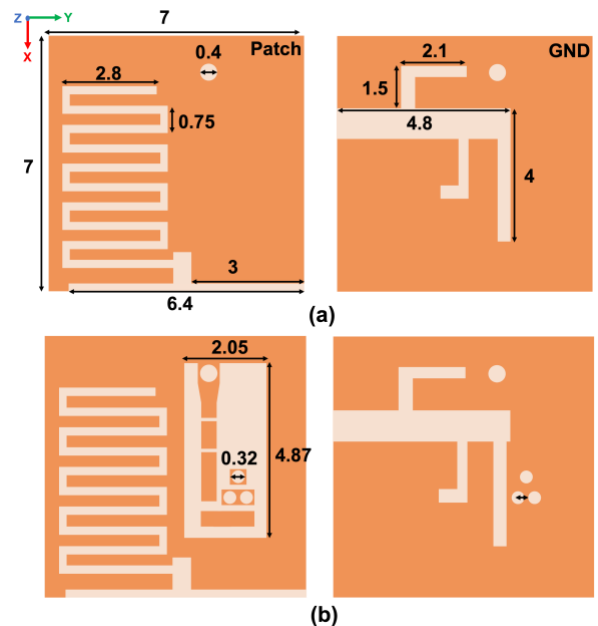


Fig. 2. Configuration of (a) the proposed antenna, and (b) the integrated rectenna

## II. IMPLANTABLE ANTENNA DESIGN

### A. Implantable Antenna Design

A single-layer patch antenna layout is designed as presented in Fig. 2 (a). The radiating patch layer and the ground layer are connected by a penetrated hole ( $x = 0.75 \text{ mm}$ ,  $y = 4.45 \text{ mm}$ ) that is filled with conductive material for feeding the antenna. The proposed antenna is mounted on a high permittivity Rogers RT/duriod 6010 substrate for the purpose of antenna miniaturization by shortening the effective wavelength of the antenna. In addition, the size of the proposed antenna is effectively reduced by embedding several meandered and open-ended slots in both radiating patch and ground layers. Therefore, the proposed antenna occupies a compact size of  $7 \text{ mm} \times 7 \text{ mm} \times 0.635 \text{ mm}^3$  and operates in the 1.4 GHz Wireless Medical Telemetry Service (WMTS: 1.395-1.432 GHz) band for wireless power delivering. To overcome the size restrictions of the implantable antenna and rectifier, we provide an ultra-miniaturized rectenna structure, as shown in Fig. 2 (b). The overall volume of the integrated rectenna is the same as that of the proposed implantable antenna without compromising its performance.

TABLE I. COMPARISON OF IMPLANTABLE RECTENNA FOR WIRELESS POWERING IN LITERATURE

Ref.	Dimensions (Antenna + Rectifier)		Resonant Frequency (For power transfer)	Gain	Biocompatible Encapsulation	Peak Efficiency	Application
[8]	$16 \times 14 \times 1.27 \text{ mm}^3$		915 MHz	-24.3 dB	Alumina	50% - 60%	Arm Implants
[9]	$\pi \times 4^2 \times 1.27 \text{ mm}^3$		915 MHz	-29.5 dBi	No	58.3%	
[10]	$12 \times 10 \times 2.04 \text{ mm}^3$		1.2 GHz	0.64 dBi	No	65% (approx.)	Wireless Pacing
[11]	$10 \times 10 \times 0.3 \text{ mm}^3$	Nan	2.45 GHz	-7.81 dBi	No	41%	Self-charging pacemaker
This work	$7 \times 7 \times 0.64 \text{ mm}^3$		1.4 GHz	-24.87 dBi	PDMS	67.9%	Wireless powering vascular implants

## B. Implantable Antenna Simulation

The proposed antenna is simulated in a multi-layer tissue phantom model by using ANSYS HFSS software. As shown in Fig. 3, a multi-layer cubic phantom is set with different electrical properties at 1.4 GHz that composes of skin (relative permittivity ( $\epsilon_r$ ) of 39.66 and a conductivity ( $\sigma$ ) of 1.03 S/m), fat ( $\epsilon_r = 1.15$ ,  $\sigma = 0.14$  S/m), and muscle ( $\epsilon_r = 54.11$ ,  $\sigma = 1.14$  S/m). However, the Rogers RT/duriod 6010 material is not biocompatible, we have insulated the proposed antenna within a filled Polydimethylsiloxane (PDMS) encapsulation with a dimension of  $8 \times 8 \times 1.635$  mm<sup>3</sup> for the simulation. Fig. 4 compares the simulated reflection coefficient ( $S_{11}$ ) of the initial antenna, the integrated rectenna, and the optimized rectenna designs. The proposed antenna shows a decent  $S_{11}$  value of -36.68 dB at 1.4 GHz. The resonant frequency shifted to 1.38 GHz with an attenuated  $S_{11}$  value of -25.2 dB after the rectifier layout fused to the antenna design. By etching the optimized slots in the ground plane,  $S_{11}$  is decreased to -41.92 dB at 1.4 GHz with a peak far-field gain value of -24.9 dBi.

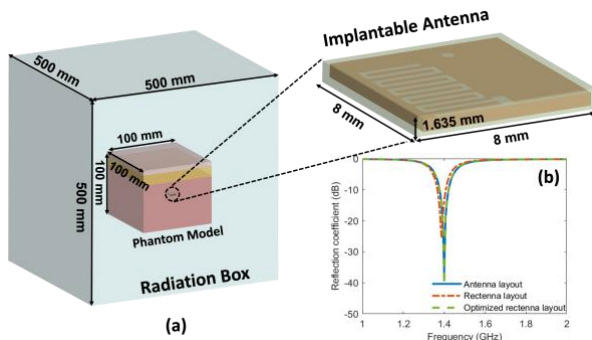


Fig. 3. (a) Antenna simulation set-up, (b) reflection coefficient results in comparison of different antenna/rectenna layouts.

## III. IMPEDANCE MATCHING AND RECTIFIER CIRCUITS DESIGN

### A. Impedance Matching and Rectifier Circuits Design

Once the receiving antenna collects the RF power, the rectifier circuit will extract and convert the RF power to DC power. However, the received RF signal is possibly attenuated as it transfers from the antenna to the rectifier, and consequently deteriorates the efficiency of the energy harvesting system. Hence, the impedance matching network plays a vital role in mitigating power loss because of impedance mismatch. In addition to the high-efficiency requirement of impedance-matching networks, simplification and compact size are also pursued. In this paper, we proposed

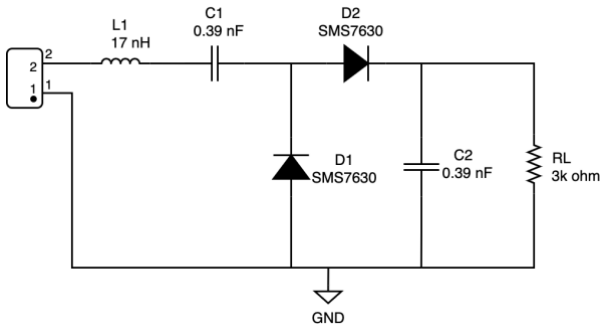


Fig. 4. Impedance matching network and rectifier circuit design.

an optimized single-matched inductor as an impedance matching network, as shown in Fig. 4.

Various rectifier topologies are employed to convert the RF signal to DC. The typical RF-to-DC rectifier topologies include half-wave rectifiers, full-wave rectifiers, voltage multipliers, and multi-stage multipliers. The choice of the rectifier depends on various factors such as the intended application and the required output voltage and power. In this paper, voltage multiplying capability and full-wave rectification are required in the rectifier circuit design to drive self-powering implantable vascular at low input power supplies. Although the output DC voltages of multiple-stage rectifiers are high, the increase in the number of stages comes at the cost of low RF-to-DC efficiency due to power losses at the diodes and results in a relatively large rectifier size. On the contrary, the rectified output generated by a shunt diode or series diode is generally lower than that of other rectifier topologies. Therefore, a voltage doubler is selected in this design to obtain a high conversion efficiency and reduce the circuit complexity. As shown in Fig. 4, a voltage doubler circuit comprises two diodes and two capacitors. The received RF input signal is rectified in the negative half cycle by forward biased diode D1 and the electric charge is stored in C1. During the positive half cycle, the diode D1 is reverse biased and D2 is forward biased charging up capacitor C2, and the charge voltage in C1 is accumulated to C2, resulting in approximately two times of the peak voltage observed at the output load. It's worth mentioning that the circuit parameters have been optimized to maximize conversion efficiency at 1.4 GHz for the received RF input power, using the inductive matching network [13].

More specifically, an essential element of the rectifier circuit is the rectifying diode, and its characteristics such as forward voltage drop, capacitance, and series resistance have a significant impact the RF-to-DC conversion efficiency. Schottky diodes are commonly preferred in rectifier circuits due to their high frequency performance and low power operations. In this work, we selected the SMS-7630 Schottky diode from Skyworks as the rectifying element. This diode features an ultra-low threshold voltage ( $V_j$ ) ranging from 0.06 V to 0.12 V, low junction capacitance and high series resistance, which is highly suitable for high frequency and low power rectifier circuits.

### B. Impedance Matching and Rectifier Circuits Simulation

The impedance matching network and the rectifier circuit was simulated using Keysight advanced design system (ADS) software. The input impedance (source) of the designed rectifier is set to  $50.672 - j3.86 \Omega$ , which was derived from the output impedance of the aforementioned implantable antenna

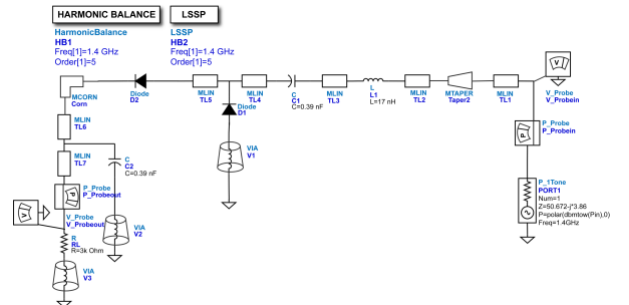


Fig. 5. Impedance matching network and rectifier circuit simulation in Keysight ADS.



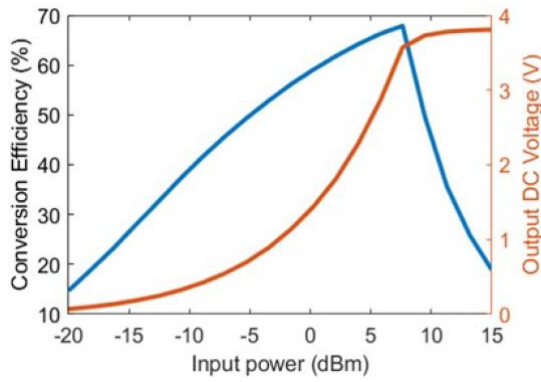


Fig. 6. Comparison of the reflection coefficient of the proposed rectifier varies with different input power levels at a resistance of 3 k $\Omega$ .

for the accurate simulation. An optimized matching inductor (L1) of 17 nH is used in this circuit to compensate for the power attenuation between the implantable antenna and the proposed rectifier. As shown in Fig. 5, the impedance of the rectifier is matched to the proposed antenna by using a tapered line feed, which favours high-impedance matching. The charge-pumping capacitors are characterized with a capacitance  $C1 = C2 = 0.39$  nF in the rectifier circuit. Fig. 6 illustrates the relationship between the simulated power conversion efficiency (PCE) and output voltage values of the rectifier with respect to the input power level under a 3 k $\Omega$  load resistor. The simulated performance of the proposed rectifier circuit was evaluated with input power ranging from -20 to 15 dBm, the maximum power conversion efficiency (PCE) of 67.9% was obtained at a power input of 7.5 dBm. Notably, the rectifier circuit exhibits a high conversion of 39.58% even at a low input power of -10 dBm. Additionally, the DC output voltage across the load exceeds 3V for input power levels higher than 6 dBm. The  $S_{11}$  values of the proposed rectifier circuit for different input power levels is presented in Fig. 7. The non-linear characteristics of the diodes result in a significant variation in impedance matching of the rectifier circuit with different input power levels. However, it can be observed that the proposed rectifier maintains good  $S_{11}$  values of below -10 dB throughout the input power range of -15 dBm to 10 dBm. In addition, an appropriate load resistance selection is also crucial for achieving optimal power conversion efficiency. Fig. 8 illustrates the conversion efficiency at various load resistances, range from 0.5 k $\Omega$  to 100 k $\Omega$  at an input power of

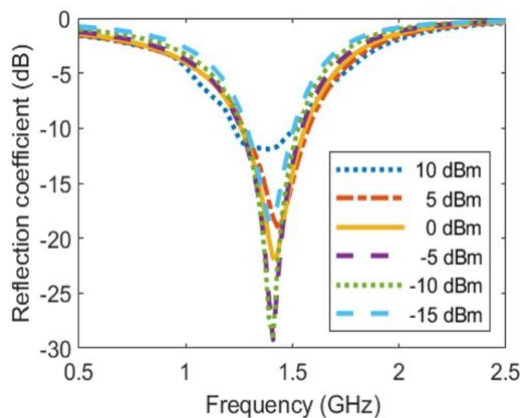


Fig. 7. Power conversion efficiency and output voltage at different input power levels.

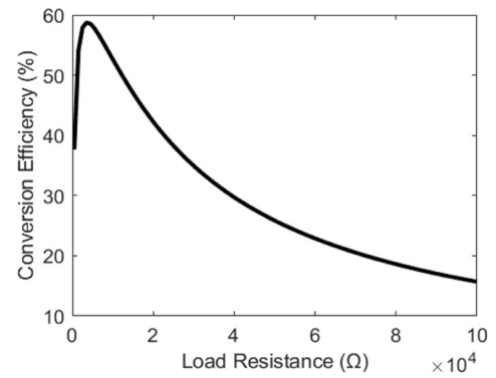


Fig. 8. Conversion efficiency versus different load resistances.

0 dBm. In consequence, the highest conversion efficiency was achieved 58.6% at a 3 k $\Omega$  load resistance.

#### IV. CONCLUSION

This study presents a highly integrated, ultra-miniaturized, and biocompatible RF rectenna with merit power conversion efficiency for the implantable vascular devices. The rectifier is fused in the implantable antenna design to achieve high compactness. At an input power of 7.5 dBm and a load resistance of 3 k $\Omega$ , the rectenna demonstrates a maximum conversion efficiency of 67.9%. In addition, the rectifier generates considerable output voltage and robust PCE across various loads and power levels. Consequently, such rectenna is desirable to compact implantable vascular devices.

#### REFERENCES

- [1] Piché, M. E., Tchernof, A., & Després, J. P. (2020). Obesity phenotypes, diabetes, and cardiovascular diseases. *Circulation research*, 126(11), 1477-1500J. Clerk Maxwell, A Treatise on Electricity and Magnetism, 3rd ed., vol. 2. Oxford: Clarendon, 1892, pp.68–73.
- [2] Giustino, G., Colombo, A., Camaj, A., Yasumura, K., Mehran, R., Stone, G. W., ... & Sharma, S. K. (2022). Coronary in-stent restenosis: JACC State-of-the-art review. *Journal of the American College of Cardiology*, 80(4), 348-372.
- [3] Cowie, M. R., & Lam, C. S. (2021). Remote monitoring and digital health tools in CVD management. *Nature Reviews Cardiology*, 18(7), 457-458.
- [4] Hoare, D., Tsiamis, A., Marland, J. R., Czyzewski, J., Kirimi, M. T., Holsgrove, M., ... & Mercer, J. R. (2022). Predicting Cardiovascular Stent Complications Using Self - Reporting Biosensors for Noninvasive Detection of Disease. *Advanced Science*, 9(15), 2105285.
- [5] Zhang, J., Das, R., Hoare, D., Wang, H., Ofiare, A., Mirzai, N., ... & Heidari, H. (2023). A Compact Dual-band Implantable Antenna for Wireless Biotelemetry in Arteriovenous Grafts. *IEEE Transactions on Antennas and Propagation*.
- [6] Zhang, J., Hoare, D., Das, R., Holsgrove, M., Czyzewski, J., Mirzai, N., ... & Heidari, H. (2022, October). Wireless Impedance Platform for Autonomous Vascular Implantable Devices. In *2022 29th IEEE International Conference on Electronics, Circuits and Systems (ICECS)* (pp. 1-4). IEEE.
- [7] Zhang, J., Das, R., Zhao, J., Mirzai, N., Mercer, J., & Heidari, H. (2022). Battery - Free and Wireless Technologies for Cardiovascular Implantable Medical Devices. *Advanced Materials Technologies*, 7(6), 2101086.
- [8] Bakogianni, S., & Koulouridis, S. (2019). A dual-band implantable rectenna for wireless data and power support at sub-GHz region. *IEEE Transactions on Antennas and Propagation*, 67(11), 6800-6810.
- [9] Xu, C., Liu, X., & Li, Z. (2020, August). Miniaturized implantable rectenna for far-field wireless power transfer. In *2020 9th Asia-Pacific Conference on Antennas and Propagation (APCAP)* (pp. 1-2). IEEE
- [10] Asif, S. M., & Braaten, B. D. (2016, June). Design of a compact implantable rectenna for wireless pacing applications. In *2016 IEEE*

International Symposium on Antennas and Propagation (APSURSI) (pp. 167-168). IEEE.

- [11] Saha, P., Mitra, D., & Parui, S. K. (2022). A circularly polarized implantable rectenna for self-charging pacemaker. *Journal of Electromagnetic Waves and Applications*, 36(11), 1576-1588.
- [12] Basir, A., & Yoo, H. (2020). Efficient wireless power transfer system with a miniaturized quad-band implantable antenna for deep-body multitasking implants. *IEEE Transactions on Microwave Theory and Techniques*, 68(5), 1943-1953.
- [13] M. Wagih, A. S. Weddell and S. Beeby, "Omnidirectional Dual-Polarized Low-Profile Textile Rectenna With Over 50% Efficiency for Sub- $\mu$ W/cm<sup>2</sup> Wearable Power Harvesting," in *IEEE Transactions on Antennas and Propagation*, vol. 69, no. 5, pp. 2522-2536, May 2021, doi: 10.1109/TAP.2020.3030992.